Available online at www.eccomasproceedia.org
Eccomas Proceedia COMPDYN (2023) 3433-3444

ECCOMAS
Proceedia

COMPDYN 2023
9th ECCOMAS Thematic Conference on
Computational Methods in Structural Dynamics and Earthquake Engineering
M. Papadrakakis, M. Fragiadakis (eds.)
Athens, Greece, 12-14 June 2023

Machine Learning Approach for Predicting Flexural Behavior Variations of I-Shaped Steel Beams due to Manufacturing Tolerances

Cyrus Eshaghi [1*], Arefeh Mazarei[2], Rui Carneiro de Barros [1], Xavier Romão [1] and José Miguel Castro [1]

[1] *Construct, Faculty of Engineering University of Porto, 4200-465 Porto, Portugal*
up202010595@up.pt

[2] *INESCTEC, Campus of faculty of Engineering of University of Porto, 4200-465 Porto Portugal*

Abstract

The main subject of this paper is the impact that manufacturing tolerances have on the cyclic performance of steel beams constructed with European I-shaped profiles, particularly in moment-resisting frames (MRF). The paper also examines the effectiveness of AL models in anticipating this behavior. Past research has shown that the behaviour of a structural steel member in bending is greatly affected by the variability of geometrical and material parameters. Most previous research that focused on the cyclic behaviour of MFR members used the nominal sections in their research, however regarding the geometry, in Europe, hot-rolled profiles, are produced with dimension tolerances that are specified and limited in the European standard EN 10034. In this research, a numerical study was performed to evaluate the influence of geometrical variability on the strength and deformation capacity of steel beams subjected to cyclic flexural loading conditions. For this purpose, an advanced finite element model was developed in Abaqus and validated against experimental test data. A parametric study was conducted in which the geometrical dimensions of the beam were considered as random input. Probabilistic distributions derived from experimental data were defined for each of the 6 random input variables associated with the cross-section dimensions. Then a total set of 1600 samples were generated using Latin Hypercube sampling for a range of profiles (IPE300 to IPE600) with different lengths to evaluate the effect of dimension tolerances on the behaviour of beams. The results showed that the variability in beam behaviour is significant and can cause over strength or reduced ability of steel members to deform under load, resulting in less ductile behaviour. Then using AI techniques, some models developed to predict maximum moment and rotation capacity of beams. Various models were evaluated, including nonlinear and linear regression analysis, neural network, decision tree, and random forest.

Keywords: Manufacturing Tolerance, Machine learning, Cyclic Loading, Rotation Capacity, Seismic Moment Resisting Frames, Steel

ISSN:2623-3347
Peer-review under responsibility of the organizing committee of COMPDYN 2023.
doi: 10.7712/120123.10650.20816

1 Introduction

The latest international codes encourage the use of advanced numerical modeling and design checks for a thorough seismic assessment of structures. In particular, nonlinear structural analysis that employs concentrated plasticity phenomenological models is effective in simulating the flexural behavior of steel beams subjected to large deformation. However, the accuracy and acceptance criteria of these models heavily rely on the rotation and bending strength parameters utilized, which need to be calibrated based on experimental results or advanced finite element models that accurately replicate the physical behavior of the structural component.

Several studies have suggested various parameters for nonlinear modeling that could be utilized for the calibration of concentrated plasticity models. For example, Lignos and Krawinkler [1] established empirical equations for estimating plastic rotations prior to and after capping, as well as the rate of cyclic deterioration in special moment connection tests. Additionally, they provided quantitative information for determining moment capacity at capping and residual moment after cyclic deterioration. Araujo et al. [2] proposed empirical equations for estimating plastic rotations in steel beam-columns with European profiles subjected to monotonic and cyclic loading. Mohabeddine et al. [3] derived an empirical equation for estimating rotation capacity in steel beams with European profiles, which can be utilized as acceptance criteria for performance-based assessment of structures or for calibration purposes in push-over analysis. Lignos et al. [4] suggested modeling criteria for the first-cycle envelope and monotonic backbone curves of steel wide-flange columns, which can be employed in nonlinear static and dynamic frame analyses. Previous studies that have examined the cyclic behavior of steel moment resisting frame components have primarily been based on nominal geometric dimensions provided by manufacturers. However, actual cross sections often deviate considerably from the nominal dimensions, as outlined by the tolerance limit deviations specified in the EN 10034:1993 standard [5]. Furthermore, while the standard provides acceptable intervals for section width, height, and thickness, the local slenderness of the plates within those intervals can vary significantly for a given profile. Since local slenderness is a critical factor in the flexural behavior of steel beams subjected to large deformation, understanding the extent of this effect is crucial.

Several researchers have explored the impact of these types of geometrical imperfections on the design and load-carrying capacity of steel members subjected to monotonic loading, including Byfield and Nethercott [6], Melcher et al. [7], and Kala et al. [8]. However, to the authors' knowledge, no studies have examined the impact of cross section dimension variability on the cyclic behavior of steel beams. While existing experimental tests may include these effects, large numbers of tests would be required to identify the effect of these imperfections, making such an approach infeasible.

Therefore, this study conducted 1600 finite element simulations in ABAQUS of cantilever beams (IPE300-IPE600) subjected to cyclic loading to investigate the effect of manufacturing tolerances on the rotation capacity of beams.

2 Methodology

This study aims to examine the impact of manufacturing tolerances on the cyclic behavior of steel flexural members with I-shaped cross-sections. To achieve this, a high-fidelity finite element model is created using ABAQUS software and the standardized SAC loading protocol is adopted. The model is a cantilever beam, assumed to represent the beam's behavior from one

end to the mid-point of inflection. This approach is commonly used in experimental and numerical studies. The study focuses on IPE300 to IPE600 profiles, which are widely used in practice, and considers a member with a length of 2, 2.5, 3, 3.5m. Figure 1 shows a 3D schematic view of the model with one edge fully restrained in all 6 degrees of freedom to ensure fixed boundary conditions. The cyclic loading is applied on the other edge, which is restrained in the X-X direction to prevent out-of-plane displacements at the top of the specimen.

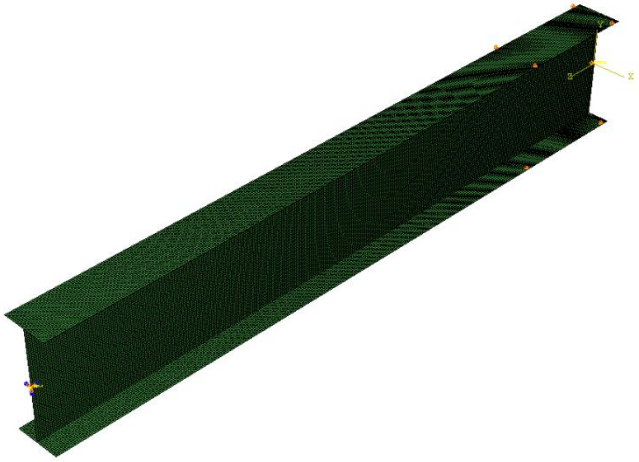

Figure 1: Beam model in Abaqus.

To avoid too much LTB, lateral restrictions were added in the flanges. According to ANSI/AISC 341-16 [23], the unbraced length (L_b), which is the distance between the lateral restraints, was calculated using Eq. 1

$$L_b = 0.095 i_z \frac{E}{F_y} \tag{1}$$

where i_z is the radius of gyration of the cross-section, E is the young modulus, F_y is the yield stress obtained from coupon tests.

$$\sigma^0 = \sigma|_0 + Q_\infty(1 - e^{-be^{pl}}) \tag{2}$$

In equation (2), the term σ^0 represents the alteration in the yield surface size as a function of equivalent plastic strain e^{pl}. The yield stress at zero equivalent plastic strain is represented by $\sigma|_0$, while Q_∞ indicates the maximum change in the yield surface size. parameter b describes the rate at which the yield surface size changes as plastic strain increases. The nonlinear kinematic hardening component involves the movement of the yield surface in the stress space through the vector backstress α, which is used to capture complex phenomena like the Bauschinger effect. Equation (3) represents the backstress evolution law, which is a mathematical expression of the vector function that shifts the center of the Mises yield surface.

$$\dot{\alpha_k} = C_k \frac{1}{s^0}(\sigma - \alpha)\dot{\bar{e}}^{pl} - \gamma_k \alpha_k \dot{\bar{e}}^{pl} \tag{3}$$

Where C_k and γ_k are material parameters calibrated from stabilized cycle, σ is the stress matrix, $\dot{\alpha_k}$ is the evolution of the back stress, and $\dot{\bar{e}}^{pl}$ is the equivalent plastic strain rate. The subscript

$''_k''$ defines the backstress number. The constitutive parameters for this model were obtained through an optimization process using data from Chen et al.'s coupon test [14]. A comparison between the coupon test and the Voce-Chaboche model is illustrated in Figure 2, and Table 1 lists the parameters used to describe the constitutive model. The finite element model was then validated against various experimental tests on different members, and the outcomes are depicted in Figure 2.

Table 1 Nonlinear Isotropic and Kinematic hardening parameters.

Material	σ|0 (N/mm2)	Q∞ (N/mm2)	b	C (N/mm2)	γ
Q355b/S355	285	69	2.86	14238	96.15

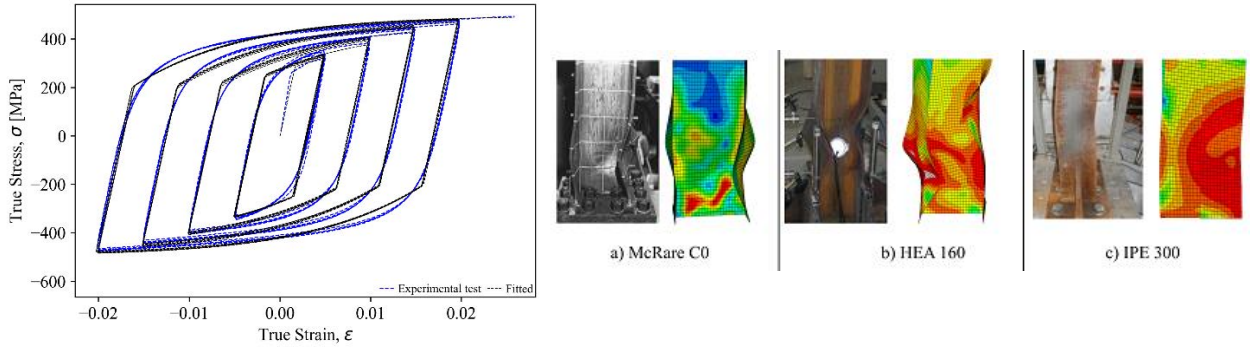

Figure 2: comparison between the buckling behavior simulated in the numerical model and from the numerical model: (a) anti-symmetric local buckling Specimens C0 (McRae[16]); (b) non-symmetric local buckling of HEA160 (D'Aniello et al [12]); (c) lateral buckling of IPE 300 (D'Aniello et al [12]).

3 Considering the dimension characteristics variability

Table 2 presents the tolerances on the shape dimensions of I and H sections of structural steel, as specified by the European standard [5]. The descriptions of the profile dimensions are illustrated in Figure 3 and their meanings are explained in Table 2.

Table 2-Dimensional tolerance for structural steel I and H sections (EN 10034:1993) (units in mm)

Section Height (h)		Flange Width (b)		Web Thickness (t_w)		Flange Thickness (t_f)	
h<=180	+3 -2	b<=110	+4 -1	t_w<7	±0.7	t_f<6.5	+1.5 -0.5
180<h<=400	+4 -2	110<b<=210	+4 -2	7=< t_w <10	±1	6.5=<t_f<10	+2 -1
400<h<=700	+5 -3	210<b<=325	+4 -4	10=< t_w <20	±1.5	10=<t_f<20	+2.5 -1.5
h>700	+5 -5	b>325	+6 -5	20=< t_w <40	±2	20=<t_f<30	+2.5 -2
				40=< t_w <60	±2.5	30=< t_f <40	+2.5 -2.5
				60< t_w	±3	40=< t_f <60	+3 -3
						60< t_f	+4 -4

Table 3 Relative statistical geometric characteristics and Correlation matrix of geometric characteristics [7]

Quantity	Mean	Standard deviation	Skewness	Kurtosis	Min Value	Max value
h	1.001	0.00443	-0.4063	3.0150	0.989	1.013
b_1	1.012	0.01026	-0.3939	4.239	0.975	1.049
b_2	1.015	0.00961	-0.5448	3.887	0.975	1.037
t_1	1.055	0.04182	1.0545	7.4730	0.949	1.3
t_{21}	0.988	0.04357	-0.2991	2.663	0.880	1.094
t_{22}	0.998	0.04803	0.3303	2.766	0.858	1.129

Quantity	h	b_1	b_2	t_1	t_{21}	t_{22}
h	1	-0.0068	0.0534	0.0399	-0.0686	-0.0989
b_1	-0.0068	1	0.6227	- 0.214	-0.2681	-0.1456
b_2	0.0534	0.6227	1	-0.2132	-0.1596	-0.0423
t_1	0.0399	-0.214	-0.2132	1	0.2368	0.2451
t_{21}	0.0686	-0.2681	-0.1596	0.2368	1	0.7634
t_{22}	-0.0989	-0.1456	0.0423	0.2451	0.7634	1

Table 2 shows that the code allows for significant variation in width and height, and reductions in thicknesses, which can greatly affect the slenderness ratios and overall performance of the profile. The coefficient of variation for geometric imperfections is based on research from the 1970s, but some studies have questioned whether these estimates are still valid due to advancements in manufacturing methods [6]. Melcher et al. [7] conducted experimental research on Czech steel hot rolled IPE profiles, and statistically evaluated the geometrical characteristics of the cross-section dimensions, as presented in Table 3. This study used the results from those tables to define the next steps in the paper.

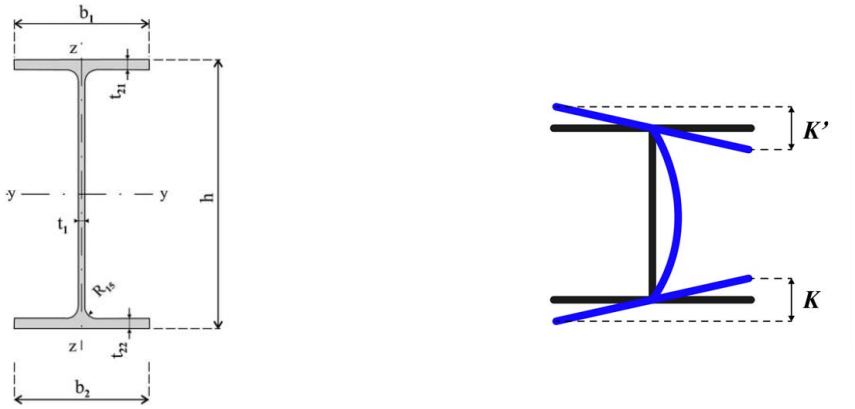

Figure 3: IPE profiles according to EN1993-1-1 and imperfection according to EN 10034:1993

As seen in Fig. 3, h is the height of the beam, b_1, b_2 are the top and bottom flange widths, t_1 is the web thickness, and t_{21}, t_{22} are the top and bottom flange thicknesses.

4 Stochastic Model

Latin hypercube sampling (LHS) is a statistical technique used to generate a nearly random set of parameter values from a multidimensional distribution. This study employs the LHS method to define the random geometries for finite element analysis. The LHS method is computationally efficient compared to standard Monte Carlo sampling since it reduces the number of samples significantly. However, the results of LHS sections are dependent on whether the components of X (variables) are independent or dependent. In this paper, a procedure for producing Latin hypercube samples is used based on a correlation matrix of geometric characteristics, as presented in Table 4, since section variables are dependent. An experimental distribution is defined to capture the true distribution of the variables.

For each profile considered in this study, 50 samples with varying dimensions are generated using the LHS method and this process repeated for 4 different lengths of each profile. The different variations of an IPE300 are illustrated in Figure 4

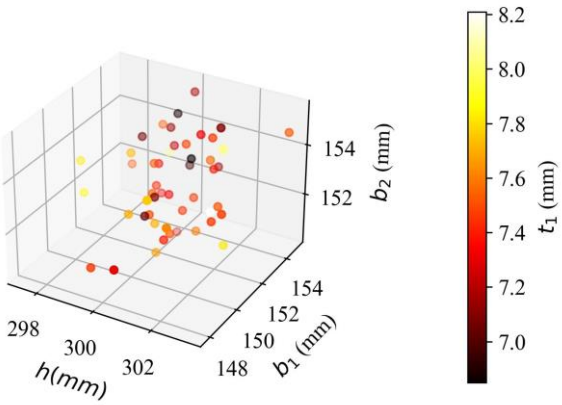

Figure 4 Latin hypercube sampling for IPE300

5 Results and Discussion

Figure 5 displays two graphs illustrating the behavior of IPE300 profiles, specifically the cyclic moment-rotation curve and the first cycle envelope, which is determined by moment and rotation values at yielding, maximum moment, and an 20% reduction in strength (M_80%). Figure 6 shows the first cycle curves for IPE300 to IPE600, based on 50 samples for the profile. The results indicate that changes in the dimensions of the beams significantly affect their strength and rotation capacity. The average first cycle curve is similar to the nominal cross section curve, but the average strength shows a higher maximum moment when the strength begins to drop. However, higher strength can increase the over-strength factor, which is not desirable for seismic design which can decrease the seismic performance of the structure. These results could be useful for reliability analysis and risk assessment, considering the variability of input modeling parameters.

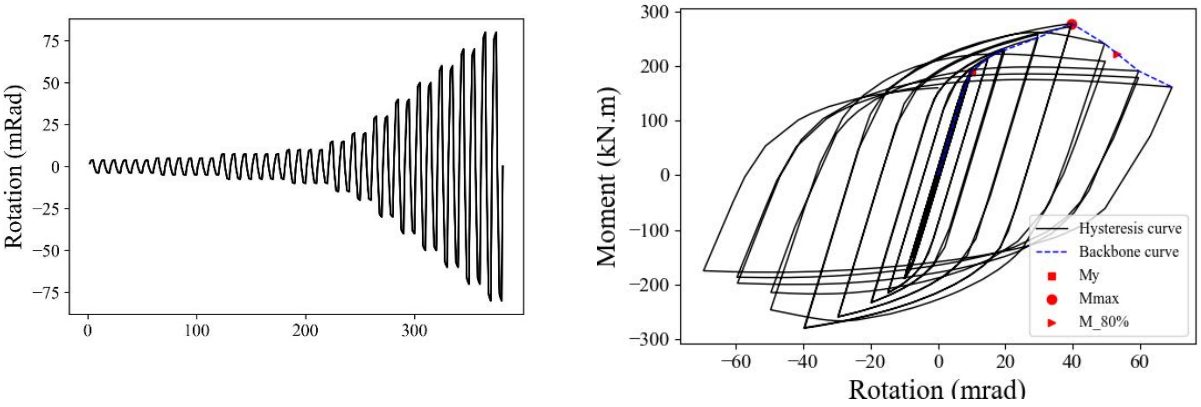

Figure 5: SAC protocol and cyclic hysteresis moment-rotation curves with first cycle curve of IPE300.

The rotation at of strength drop ($\theta_{80\%}$) is widely accepted as the parameter that defines the rotation capacity of the beam when subjected to large deformation.

Figure 6 illustrates the diversity of the $\theta_{80\%}$ values for various profiles with a length of 2 meters. The manufacturing tolerances in the dimensions of the cross-section have a significant impact on the variability of the data. In addition, Figure 6 demonstrates that there is greater variation in profiles with lower heights compared to those with higher heights. This is because the impact of tolerance on a slenderer profile is greater.

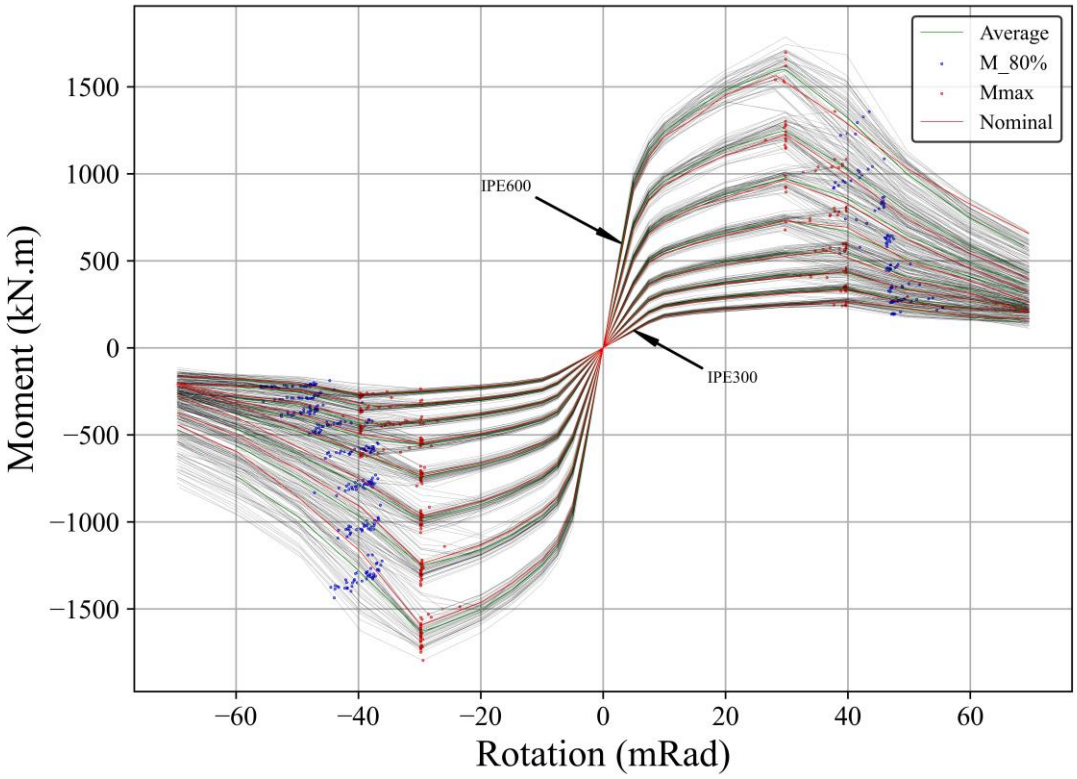

Figure 6: backbone curves of IPE300 to IPE600 and the impact of dimension tolerances on parameters

5.1. Strong beam, Weak column

The problem of "strong beam, weak column" in seismic design refers to a situation where the beams of a structure are much stronger than the columns. In this scenario, during a seismic event, the beams can cause the columns to fail due to the high forces that are transmitted through them.

The strong beam, weak column problem is a critical issue in seismic design because it can result in catastrophic failure of the structure, leading to loss of life and property damage. To avoid this problem, seismic design standards typically require that the strength and stiffness of the beams and columns be balanced to ensure that they work together to resist seismic loads.

According to the findings of this study, there is a high likelihood of overstrength for various profiles of different lengths, as demonstrated by the graph in figure 6.

The following section involved creating several models using machine learning methods to predict the maximum moment and rotation capacity and evaluating the accuracy of these models. Moreover, an empirical equation was developed to predict the rotation capacity at maximum moment and when the maximum moment has decreased by 20%. Several models

were evaluated, including nonlinear regression, linear regression analysis, neural network, decision tree, and random forest, with the aim of achieving the desired outcome. To evaluate the models, 80% of the data was used for training, while the remaining 20% was used for testing. Additionally, the training data was divided into two sets: a training set and a validation set, which were used to optimize the hyperparameters of the models under consideration.

5.2. nonlinear regression analysis

Nonlinear regression analysis requires careful consideration of the model assumptions, such as the distribution of errors, and the choice of model and parameters can have a significant impact on the results. It is important to evaluate the fit of the model to the data, often using diagnostic plots or statistical tests, to ensure that the model is appropriate, and the results are reliable. Current construction steels can develop large deformation without loss of strength. The rotation capacity of a steel member depends strongly on geometrical instabilities. Flange and web slenderness present the major influencing parameters of a given plated beam. Therefore, an empirical equation based on nonlinear regression analysis to estimate rotations corresponding to maximum moment and 20% drop in maximum moment of all the profiles is presented in Eq. 4.

$$\theta_{80\%} = a\left(\frac{L}{h}\right)^{b}\left(\frac{hw}{t_w}\right)^{c}\left(\frac{b_f}{2t_f}\right)^{d} \tag{4}$$

Where $\frac{h}{t_w}$ represent the web slenderness and $\frac{b}{2t_f}$ represent flange slenderness. The following are the regression coefficients:

Dataset	a	b	c	d
All data	889.56	0.39	-0.75	-0.56

L length of cantilever beam
t_f flange thickness
t_w web thickness
h beam depth
b_f flange width
L_b unbraced length.
i_z radius of gyration

There is a strong correlation between measured and anticipated results.

The study examined three methods to assess the precision of the models, which were absolute error, mean square error, and r square. The equation 5 and 6 in the study describes these methods.

$$\text{MAE} = \frac{1}{n} * \sum\left|y_{pred} - y_{true}\right| \tag{5}$$

$$\text{MSE} = \frac{1}{n} * \sum(y_{pred} - y_{true})^2 \tag{6}$$

n is the number of samples in the dataset
y_{true} is the predicted value of the model.
y_{true} is the true value of the target variable.

The proposed equation underwent extensive research before being suggested, as indicated by the mean absolute error of 1.05 and the mean squared error of 1.8 in the nonlinear regression. However, when attempting to estimate the maximum moment of beams, there was unacceptable inaccuracy, as evidenced by the R^2 correlation of 0.78 and the following error values, mean absolute error of 146.29 and mean squared error of 41669.38. The benefit of this approach is that we arrive at a final equation that researchers and engineers may utilize with ease.

5.3. Linear regression

The linear regression method is widely used in civil engineering to model the relationship between various factors affecting the performance of structures, such as load-bearing capacity, deflection, and durability. In this part a liners regression model developed to predict $\theta_{80\%}$ and θ_{max} and M_{max}. The mean squared error of the linear regression for predicting $\theta_{80\%}$ is 2.04. R-Square for the test set is 0.94 and 1.12 means absolute error from this model.

5.4. Neural networks

Neural networks are a type of machine learning model that is inspired by the structure and function of the human brain. They consist of layers of interconnected nodes, also known as neurons, which process and transmit information using mathematical functions.

In this part a liners regression model developed to predict $\theta_{80\%}$ and θ_{max} and M_{max}. The neural network's mean squared error for $\theta_{80\%}$ is 0.77. The neural network's mean absolute error is 0.64 and R-Square for the test set is 0.98

5.5. Decision tree

Decision trees are a versatile tool that can be used for both classification and regression problems. When applied to regression analysis, decision trees aim to predict continuous target variables by dividing the feature space into smaller subsets based on input feature values [22].

The authors of the paper utilized decision tree analysis to predict the variables of interest, and the resulting metrics indicated a mean squared error of 3.09 and a mean absolute error of 1.21. The testing set R-squared value was found to be 0.91.

5.6. Random forest

Random forest is a powerful machine learning algorithm that can be used for both classification and regression tasks. In regression, the goal is to predict a continuous target variable, and random forest is particularly well-suited for this task because it can capture complex nonlinear relationships between input features and the target variable.

Random forest has several advantages for regression, such as its ability to handle high-dimensional data and outliers, and its ability to capture complex nonlinear relationships between the input features and the target variable. Additionally, the importance of input features can be easily interpreted based on their contribution to the variance reduction in the individual decision trees.

The study utilized random forest regression analysis to predict the variables of interest. The results revealed that the mean squared error was 1.98 and the mean absolute error was 0.94. The R-squared value for the testing set was determined to be 0.94.

By repeating the previous analysis for predicting maximum moment, we can obtain more encouraging outcomes. Even though the R-squared value is almost 1, non-linear regression still

produces substantial mean absolute and mean squared errors. The results of this section show that the neural net's mean squared error is 15.20 and the mean absolute error is 2.19, while the linear regression's mean squared error is 1503.04 and the mean absolute error is 32.30. The testing set R-squared values for the neural net and linear regression are 0.9999 and 0.9908, respectively. Moreover, the decision tree has a mean squared error of 156.43 and a mean absolute error of 8.53, with a testing set R-squared value of 0.9991. Finally, Random Forest has a mean squared error of 122.08 and a mean absolute error of 7.11, with a testing set R-squared value of 0.9993.

Conclusion

The primary focus of this study was to examine how manufacturing dimensional tolerances impact the flexural behavior of steel beams when subjected to cyclic loading. To accomplish this objective, the study conducted 1600 analyses on eight distinct steel profiles, ranging from IPE300 to IPE600. After evaluating the results, the study found that this tolerance has a significant effect and can potentially cause either overstrength or a reduction in the rotation capacity of steel beams in MRF. Therefore, future design and analysis of steel structures should give greater consideration to this geometrical imperfection.

In this study, various techniques such as linear regression, nonlinear regression analysis, neural network, decision tree and random forest, were employed to predict the maximum moment and rotation at maximum moment and 20% of maximum moment. The findings suggest that neural network models are more accurate in predicting both variables, making it a reliable approach for predicting moment and rotation. It is interesting to note that utilizing a neural network can be highly beneficial in this context since running a model with Abaqus can be both time-consuming and expensive.

Acknowledgements

This paper has been prepared within the scope of the Project “SD Poles - Steel and Dampers for Poles” with reference POCI-01-0247-FEDER-039865, co-financed by European Regional Development Fund (ERDF) through the Operational Program for Competitiveness and Internationalization (COMPETE 2020) under the PORTUGAL 2020, of which the first author is a grantee. This work is also integrated in the R&D activities of the CONSTRUCT Institute on Structures and Constructions (Instituto de I&D em Estruturas e Construções), financially supported by Base Funding UIDB/04708/2020 through national funds of FCT/MCTES (PIDDAC).

REFRENCES

[1] Lignos, D.G.; Krawinkler, H.; (2011) *Deterioration Modeling of Steel Components in Support of Collapse Prediction of Steel Moment Frames under Earthquake Loading.* Journal of Structural Engineering. **137**(11): p. 1291-1302.

[2] Araújo, M.; Macedo, L.; Castro, J.M.; (2017) *Evaluation of the rotation capacity limits of steel members defined in EC8-3.* Journal of Constructional Steel Research. **135**: p. 11-29.

[3] Mohabeddine, A.; Koudri, Y.W.; Correia, J.A.F.O.; Castro, J.M.; (2021) *Rotation capacity of steel members for the seismic assessment of steel buildings.* Engineering Structures. **244**: p. 112760.

[4] Lignos, D.G.H.; Elkady, A.; Deierlein, G.G.; (2019) *Proposed Updates to the ASCE 41 Nonlinear Modeling Parameters for Wide-Flange Steel Columns in Support of Performance-Based Seismic Engineering.* Journal of Structural Engineering. **145**(9): p. 04019083.

[5] Standards, B., *BS EN 10034:1993 Structural steel I and H sections Tolerances on shape and dimensions*. (1993).

[6] Byfield, M. P.; Nethercot, D A.; (1997) *Material and geometric properties of structural steel for use in design.* The Structural Engineer. **75**(25).

[7] Melcher, J.K., Z. Holicky´, M. Fajkus, M. Rozlı ´vka, L. . (2004) *Design characteristics of structural steels based on statistical analysis of metallurgical products.* Journal of Constructional Steel Research. **60**(3-5): p. 795-808.

[8] KALA, Z.; Kala, J.; (2005) *Sensitivity analysis of lateral buckling stability problems of hot-rolled steel beams.* Slovac Journal of Civil Engineering. **2**: p. 9-14.

[9] Mohabeddine, A.I.; Eshaghi, C.; Correia, José A.F.O.; Castro J. M. (2022) *Analytical investigation of the cyclic behaviour of I-shaped steel beam with reinforced web using bonded CFRP.* Steel and Composit Structures. **43**(4): p. 447-456.

[10] Kato, B.; (1989) *Rotation capacity of H-section members as determined by local buckling.* Journal of Constructional Steel Research. **13**(2-3): p. 95-109.

[11] Kato, B.; Nakao, M.; (1994) *Strength and deformation capacity of h-shaped steel members governed by local buckling.* Journal of Structural and Construction Engineering (Transactions of AIJ). **59**(458): p. 127-136.

[12] D'Aniello, M. .;Landolfo, R. .;Piluso, V.Rizzano, G.; (2012) *Ultimate behavior of steel beams under non-uniform bending.* Journal of Constructional Steel Research. **78**: p. 144-158.

[13] Cheng, X.; Chen, Y.; (2018) *Ultimate strength of H-sections under combined compression and uniaxial bending considering plate interaction.* Journal of Constructional Steel Research. **143**: p. 196-207.

[14] Chen, Y.; Wei, S.;Tak-Ming, C. (2014) *Cyclic stress-strain behavior of structural steel with yieldstrength up to 460 N/mm2.* Frontiers of Structural and Civil Engineering. **8**(2): p. 178-186.

[15] Mohabeddine, A. I.; Kuidri, Y.W.; Castro, J. M.; Correia, J. A. F. O.; *Numerical Simulation and Calibration of the Cyclic Behavior of Structural Steel Under Different Loading Protocols*, in *XIX International Colloquium on Mechanical Fatigue of Metals*. (2018): Porto, Portugal. p. 97–98.

[16] MacRae, G.A.; *The seismic response of steel frames," University of Canterbury Christchurch*, in *Civil Engineering*. (1989), University of Canterbury: New Zealand.

[17] CEN, *Eurocode 3: Design of steel structures-part 1.1: General rules and rules for buildings*, in *CEN, European Committee for Standardization*. (1992).

[18] McKay, M.D.; R. J. Beckman, W. J. Conover. (1979) *A Comparison of Three Methods for Selecting Values of Input Variables in the Analysis of Output from a Computer Code.* Technometrics 21. **2**: p. 239-45.

[19] Tang, B.; (1988) *Orthogonal Array-Based Latin Hypercubes.* Journal of the American Statistical Association. **88**: p. 1392–1397.

[20] Anders M. J. Olsson, G.E.S.; (2002) *Latin Hypercube Sampling for Stochastic Finite Element Analysis.* Journal of Engineering Mechanics. **128**(1).

[21] Stein, M.; (1987) *Large Sample Properties of Simulations Using Latin Hypercube Sampling.* Technometrics. **29**(2): p. 143-151.

[22] Witten, I. H.; Frank, E.; Hall, M. A. (2011) Data Mining: Practical Machine Learning Tools and Techniques (3rd edition).

[23] Breiman, L. (2001). Random forests. Machine learning. 45(1): p. 5-32.